

ORIGINAL RESEARCH

# Evaluation of Biventricular Functions in Transplanted Hearts Using 3-Dimensional Speckle-Tracking Echocardiography

Qing Lv, MD, PhD\*; Wei Sun, MD\*; Jing Wang, MD, PhD; Chun Wu, MD, PhD; He Li, MD, PhD; Xuehua Shen, MD; Bo Liang, MD; Nianguo Dong, MD, PhD; Yuman Li, MD, PhD,\*\* Li Zhang, MD, PhD;\*\* Mingxing Xie, MD, PhD\*\*

**BACKGROUND:** The current study aims to validate the accuracy of 3-dimensional speckle-tracking echocardiography (3D-STE) in evaluating biventricular functions against the accuracy of cardiac magnetic resonance (CMR) and to explore the comprehensive characteristics and normal values for 3D-biventricular functions in transplanted hearts.

**METHODS AND RESULTS:** A cohort of 35 heart transplant (HT) patients underwent both 3D echocardiography and CMR examination to validate the accuracy of 3D-STE in evaluating biventricular functions (Protocol 1). Then, 3D-STE derived biventricular functions were compared between 46 HT patients and 46 non-HT controls (Protocol 2). Protocol 1, validated that 3D-STE showed excellent accuracy in evaluating biventricular functions of transplanted hearts against CMR. Protocol 2, revealed lower (normal range) 3D-biventricular ejection fractions in HT patients than in controls ( $P<0.001$ ). 3D-left ventricular global longitudinal strain, left ventricular-global circumferential strain, left ventricular-global radial strain, left ventricular-global performance index and right ventricular free-wall longitudinal strain were all lower in the HT patients than in healthy controls ( $P<0.001$ ). Further, these strain values were all good for differentiating between groups (areas under the curve: 0.80–0.94,  $P<0.001$ ). Moreover, left ventricular-lateral-wall radial displacement was higher and septal-wall radial displacement was lower in the HT group than in control group ( $P<0.001$ ).

**CONCLUSIONS:** Compared with cardiac magnetic resonance, 3D-STE can evaluate biventricular functions of transplanted hearts accurately; 3D-biventricular mechanical functions are reduced even in clinically well HT patients. The provided characteristics and appropriate normal values of biventricular functions can be the basis for detection of ventricular dysfunction during follow-ups and further studies on transplanted hearts.

**Key Words:** biventricular function ■ cardiac magnetic resonance ■ heart transplant ■ myocardial strain ■ 3-dimensional speckle-tracking echocardiography

**H**earth transMplant (HT) is the most effective treatment for patients with end-stage heart failure, and the 1-year survival rate after HT increases to 90%.<sup>1</sup> Orthotopic HT involves factors that affect myocardial function, including injuries caused by ischemia-reperfusion, pericardiotomy surgery, and subsequent progressive remodeling after HT,<sup>2–5</sup> rendering the graft ventricular function different from healthy controls even

in healthy HT recipients. Therefore, it is unsatisfactory to use the normal values derived from non-HT healthy subjects for the HT recipients. Additionally, the ventricular function may be impaired owing to several post-operative complications that include acute rejection and cardiac allograft vasculopathy,<sup>6–8</sup> which make an evaluation of graft ventricular function clinically complicated. Therefore, it is crucial to accurately assess the

Correspondence to: Mingxing Xie, MD, PhD, Li Zhang, MD, PhD, and Yuman Li, MD, PhD, 1277 Jiefang Avenue, Wuhan, China. E-mails: xiemx@hust.edu.cn, zli429@hust.edu.cn, liym@hust.edu.cn

Supplementary Materials for this article are available at <https://www.ahajournals.org/doi/suppl/10.1161/JAHA.119.015742>

\*Dr Lv and Dr Sun are co-first authors.

\*\*Mingxing Xie, Li Zhang and Yuman Li are the co-corresponding authors.

For Sources of Funding and Disclosures, see page 9.

© 2020 The Authors. Published on behalf of the American Heart Association, Inc., by Wiley. This is an open access article under the terms of the Creative Commons Attribution-NonCommercial-NoDerivs License, which permits use and distribution in any medium, provided the original work is properly cited, the use is non-commercial and no modifications or adaptations are made.

JAHA is available at: [www.ahajournals.org/journal/jaha](http://www.ahajournals.org/journal/jaha).

## CLINICAL PERSPECTIVE

### What Is New?

- Three-dimensional speckle-tracking echocardiography shows excellent accuracy in the evaluation of biventricular functions in transplanted hearts compared with cardiac magnetic resonance.
- Three-dimensional biventricular mechanical functions are reduced in clinically well heart transplant patients compared with non-heart transplant healthy controls.

### What Are the Clinical Implications?

- The provided characteristics and appropriate normal values of 3-dimensional biventricular mechanical functions can be the basis for the accurate evaluation and detection of ventricular dysfunction in follow-up studies of transplanted hearts.

## Nonstandard Abbreviations and Acronyms

<b>2D</b>	2-dimensional
<b>3D</b>	3-dimensional
<b>2D-STE</b>	2-dimensional speckle-tracking echo cardiography
<b>3D-STE</b>	3-dimensional speckle-tracking echo cardiography
<b>CMR</b>	cardiac magnetic resonance
<b>FWLS</b>	free-wall longitudinal strain
<b>GLS</b>	global longitudinal strain
<b>GCS</b>	global circumferential strain
<b>GRS</b>	global radial strain
<b>GPI</b>	global performance index
<b>HT</b>	heart transplant
<b>STE</b>	speckle-tracking echocardiography
<b>SDI</b>	systolic dyssynchrony index

characteristics and normal values of ventricular function in follow-up studies of transplanted hearts.

Echocardiography is a convenient, valuable, and non-invasive imaging tool for assessing ventricular function during follow-up examinations in transplanted hearts. Compared with conventional echocardiographic parameters, the myocardial strain derived from speckle-tracking echocardiography (STE) can detect early changes in ventricular function with greater sensitivity, more accurately quantifying global and regional myocardial functions. With respect to 2-dimensional (2D)-STE, previous studies have identified the impaired

myocardial function and reported the normal values in clinically well HT recipients.<sup>9–11</sup> However, 2D-STE is time-consuming, and the 2D plane of interest is not always visible during the cardiac cycle. Moreover, transplanted hearts show noteworthy translational motion during the cardiac phase,<sup>12</sup> which can aggravate the “out of plane phenomenon” of 2D-STE, and the complex anatomy of the right ventricle poses another limitation for assessing true cardiac function using this technique.

Three-dimensional (3D)-STE was developed to evaluate the ventricular function in all 3 spatial dimensions, and thereby, to overcome the limitation of plane dependency existing with 2D-STE. Moreover, 3D-STE requires less time to acquire and analyze images.<sup>13</sup> Furthermore, some studies have shown that 3D-STE can accurately assess ventricular function compared with the referenced standard-cardiac magnetic resonance (CMR) both in healthy subjects and in those with various heart diseases.<sup>14–17</sup> However, to the best of our knowledge, the accuracy of 3D-STE in evaluating biventricular functions in transplanted hearts has not been validated, and neither have the normal values of 3D-biventricular mechanical functions in transplanted hearts. Therefore, this study aimed to: (1) validate the accuracy of 3D-STE in evaluating biventricular functions compared with the accuracy of CMR in transplanted hearts; and (2) define the characteristics and normal values of 3D-biventricular mechanical functions in clinically well HT patients.

## METHODS

The data that support the findings of this study are available from the corresponding author upon reasonable request.

### Study Participants

A total of 130 participants at Union Hospital in Wuhan, China, were prospectively enrolled in this study between November 2017 and March 2019.

In Protocol 1, we prospectively enrolled 42 HT recipients who underwent echocardiography at their routine follow-up examinations and also agreed to undergo CMR examination within the following 24 hours. We excluded 7 of the 42 patients because of either poor 3D-echocardiographic image quality (n=5) or failure to acquire appropriate cine-loops with CMR (n=2). The remaining 35 participants were included in the final study (27 men and 8 women; mean age, 46±13 years; a range of 6 months to 3 years after HT). Among the 35 HT recipients, 28 presented as clinically well (13 clinically well recipients at 1 year after HT also participated in Protocol 2), 4 showed acute rejection, 2 presented with cardiac allograft vasculopathy, and 1 presented

with post-transplant lymphoproliferative disease involving the pericardium.

In Protocol 2, 55 clinically well HT recipients at 1-year post-surgery were prospectively enrolled in the HT group (including 13 clinically qualifying patients from Protocol 1). The inclusion criteria were no significant acute rejection at the time of echocardiographic examination as established by biopsy, no significant coronary artery disease via angiographic evaluation, no renal failure, and 2D-echocardiography-derived left ventricular ejection fraction (LVEF) >55% and right ventricular (RV) fractional area change >35%. The exclusion criteria were uncontrolled hypertension, uncontrolled blood glucose, more than mild valvular regurgitation or stenosis combined with another heart surgery, and non-sinus rhythm. Of the 55 clinically well HT patients, 9 participants were excluded owing to insufficient image quality during strain analysis. The remaining 46 HT patients were included in this study. On the other hand, the control group consisted of 46 healthy subjects with a similar distribution of sex and age to the HT group. They had no history of hypertension, diabetes mellitus, renal failure, or other diseases. This was confirmed with physical examinations, biochemical tests, electrocardiography, and echocardiography.

This study was approved by the Ethics Committee of Tongji Medical College, Huazhong University of Science and Technology. Furthermore, we obtained written informed consent from all participants.

### Conventional 2D Echocardiography

All conventional 2D and Doppler images were acquired using a commercially available system (EPIQ 7C, Philips Medical Systems, Andover, USA). A minimum of 4 heart-beat images were collected and stored in DICOM (digital imaging and communications in medicine) format. All 2D echocardiographic parameters were acquired according to the recommendation of the American Society of Echocardiography.<sup>18</sup> LVEF was measured by the Biplane Simpson Method in 2- and 4-chamber apical views.

### THREE-DIMENSIONAL SPECKLE-TRACKING ECHOCARDIOGRAPHY

Four heartbeat LV or RV 3D full-volume images were respectively collected. The frame rates of the volumetric images were 19 to 23 MHz. The images were stored in DICOM format and analyzed offline.

After selecting images of LV full-volume with the highest quality, the 4D LV-Analysis 3.1 software (TomTec Imaging Systems, Unterschleissheim, Germany) began analysis. Once the center of the mitral annulus and apex of the left ventricle were determined from apical view, the workstation automatically

performed a contour tracking of the LV endocardium. A manual adjustment was performed in case of unsatisfactory outcomes. Values for LV-end diastolic volume (EDV), end-systolic volume (ESV), ejection fraction, and the myocardial strain, displacement, and twist function could be generated automatically by the software. The LV global longitudinal strain (GLS), global circumferential strain (GCS), global radial strain (GRS), respectively, were calculated as the average peak systolic longitudinal, circumferential, and radial strain of all 16 segments. The LV septal and lateral radial displacements were obtained by averaging the segmental values corresponding to the septal and lateral walls. The global peak systolic strain (GS), systolic dyssynchrony index (SDI), and torsion of the left ventricle were automatically generated by the software, and LV global performance index (GPI) was calculated as  $GPI = GS \times \text{torsion} \div SDI$ .<sup>19</sup> Moreover, when 3D SDI was found to be >8.3%, left ventricular dyssynchrony was defined.<sup>20</sup>

The 4D RV-Function 2.0 software (TomTec Imaging Systems, Unterschleissheim, Germany) was used for analysis following the selection of high-quality RV 3D full-volume images. The analysis was performed according to the method used by Muraru et al.<sup>16</sup> RV volumes, ejection fraction, and free-wall longitudinal strain (FWLS) were generated automatically. RV FWLS was defined as the mean longitudinal peak systolic strain of 3 segments of the RV free wall.

### Cardiac Magnetic Resonance

CMR imaging was performed using a 1.5-Tesla system (MAGNETOM Aera, Siemens Healthineers, Erlangen, Germany). Three long-axis slices (2-, 3-, and 4-chamber), and a set of contiguous short-axis cine images of the left and right ventricle were acquired with a steady-state free precession sequence during a breath-hold of 10 to 15 seconds. The cine image parameters were as follows: repetition time/echo (ms), 38.09/1.21; slice thickness, 8 mm; a field of view of 340×255 mm<sup>2</sup>; matrix, 205×256 pixels; flip angle, 80°.

Subsequently, commercial software (Argus, Siemens Healthineers) was used for image processing. Cardiac volumetric and functional parameters were derived by manual delineation of the endocardial contours on the continuous LV or RV short-axis cine images, respectively. Trabeculations and papillary muscles were carefully included in the ventricular cavity. The parameters of biventricular volume and ejection fraction were automatically generated.

### Reproducibility

Of the 35 HT recipients in Protocol 1, 15 HT patients were selected randomly to evaluate the reproducibility of 3D-STE and CMR. For intra-observer variability, analysis of the first 3D-STE and CMR data set was

repeated 2 to 4 weeks later by the same primary investigator. For inter-observer variability, the 3D-STE and CMR data were analyzed by 2 masked investigators. During all repeated analyses, investigators were masked to the results of the first measurements.

## Statistical Analysis

Normally distributed continuous data are presented as mean±SD. The normality of distribution was tested using the Shapiro-Wilk test. Categorical variables are presented as absolute numbers (percentages). In Protocol 1, 3D-STE measurements were compared with the corresponding CMR values via Pearson correlation coefficients and Bland-Altman analyses. The reproducibility of 3D-STE and CMR was assessed using intraclass correlation coefficients and Bland-Altman analyses. In Protocol 2, comparisons of variables in the HT and control groups were performed through t tests for continuous variables and Chi-square tests for categorical variables. The adjustment for heart rate in comparisons of 3D-biventricular strain values between the HT and control groups were performed via the analysis of covariance. Diagnostic accuracy of 3D-biventricular strain for detecting clinically well HT recipients was evaluated using receiver operating characteristic analysis, and the receiver operating characteristic curves were performed using a MedCalc Version 19.0.4 (MedCalc Software, Ostend, Belgium). All statistical analyses, except for the analysis of receiver operating characteristic curves, were performed using SPSS 23.0 statistical software (IBM, Armonk, NY). A  $P<0.05$  was considered statistically significant.

## RESULTS

### Accuracy of 3D-STE in Evaluating Biventricular Functions Against CMR in Protocol 1

Of the 42 participants after HT in Protocol 1, 7 patients were excluded from analysis because of poor 3D-echocardiographic image quality or failure to acquire appropriate cine-loops with CMR, remaining 35 participants included in the final analysis. There were no significant differences in patient characteristics between the included and excluded patients.

The baseline clinical characteristics of the 35 participants after HT in Protocol 1 are summarized in Table S1; 3D-STE-derived values of biventricular volumes correlated well with the corresponding CMR values ( $r=0.88, 0.92, 0.86$ , and  $0.89$  for LV EDV, LV ESV, RV EDV, RV ESV, respectively;  $P<0.001$ ). The Bland-Altman analysis revealed small negative biases of 11, 4, 13, and 8 mL for LV EDV, LV ESV, RV EDV, RV ESV,

respectively, reflecting a slight underestimation of volumes by the 3D-STE method.

With respect to parameters of the biventricular functions, a substantial correlation was determined for LVEF ( $r=0.96, P<0.001$ ) and RVEF ( $r=0.95, P<0.001$ ), and Bland-Altman analysis demonstrated a small bias and relatively narrow limits of agreement (LVEF, bias= $-0.5\%$ , limits of agreement= $-0.5\%\pm 3.7\%$ ; RVEF, bias= $0.5\%$ , limits of agreement= $0.5\%\pm 4.5\%$ ) between both techniques (Figure S1).

In addition, LV GLS, LV GCS, LV GRS by 3D-STE were all well correlated with CMR-LVEF ( $r=-0.85, -0.93, 0.90$ , respectively;  $P<0.001$ ). Moreover, 3D-STE RV FWLS correlated well with CMR-RVEF ( $r=-0.83, P<0.001$ ; Figure S2).

### Baseline Clinical Characteristics of the 46 Clinically Well HT Patients and 46 Non-HT Controls in Protocol 2

Of the 55 patients after HT in Protocol 2, 9 patients were excluded from analysis because of poor 3D-echocardiographic image quality; the remaining 46 patients were included in the final analysis. There were no significant differences in patient characteristics between the included and excluded patients.

The clinical characteristics of the 46 HT recipients are summarized in Table 1. No significant differences

**Table 1. Clinical Characteristics of the 46 HT Recipients**

Parameter	Value
Pre-HT	
Etiology for transplant	
Dilated cardiomyopathy	24 (52%)
Hypertrophic cardiomyopathy	3 (7%)
Ischemic cardiomyopathy	6 (13%)
Valvular/rheumatic heart disease	4 (9%)
Complex congenital heart disease	3 (7%)
Restrictive cardiomyopathy	1 (2%)
Other diseases	5 (11%)
Donor age at HT, y	33±11
Recipient age at HT, y	46±13
Invasive sPAP, mm Hg	55±18
Invasive mPAP, mm Hg	37±12
Parameters at echocardiographic examination	
Time since HT, y	1.0±0.1
Systolic blood pressure, mm Hg	120±8
Diastolic blood pressure, mm Hg	81±9
Comorbidities	
Hypertension	22 (49%)
Diabetes mellitus	21 (46%)

Data are expressed as mean±SD or as number (%). HT indicates heart transplant; mPAP, mean pulmonary artery pressure; and sPAP, systolic pulmonary artery pressure.



in sex, age, height, weight, body surface area, systolic blood pressure, or diastolic blood pressure were observed between the HT group and the control group. Heart rates in HT subjects were higher than those in the control group ( $P<0.001$ ; Table 2).

## Conventional 2D Echocardiographic Measurements

The 2D-LVEF and RV fractional area change were lower in the HT group compared with the controls, but still within the normal range ( $64\pm 5\%$  versus  $68\pm 4\%$ ,  $44\pm 4\%$  versus  $50\pm 4\%$ , respectively,  $P<0.001$ ). All conventional parameters of RV longitudinal systolic function (including tricuspid annular plane systolic excursion and systolic tricuspid lateral annular tissue velocity) were decreased in HT group compared with those in the control group ( $P<0.001$ ). The complete data on the comparison of 2D echocardiographic and Doppler parameters between the HT and control groups are presented in Table 2.

**Table 2. General Information and 2-Dimensional Echocardiographic Measurements of HT Group and Control Group**

Parameter	HT Group (n=46)	Control Group (n=46)	P Value
Men (%)	36 (78%)	34 (74%)	0.625
Age, y	46±13	45±13	0.538
Height, cm	168±7	168±7	0.829
Weight, kg	68±13	67±10	0.778
BSA, m <sup>2</sup>	1.7±0.2	1.7±0.2	0.970
HR, bpm	89±9	68±11	<0.001
SBP, mm Hg	119±9	117±7	0.284
DBP, mm Hg	79±9	76±8	0.203
Left ventricle			
LVEF, %	64±5	68±4	<0.001
Bicuspid E, m/s	0.9±0.2	0.8±0.1	0.004
Bicuspid A, m/s	0.5±0.1	0.7±0.2	<0.001
Bicuspid E/A ratio	1.8±0.4	1.2±0.4	<0.001
Bicuspid e', cm/s	11±2	12±3	0.519
Bicuspid E/e'	8±3	7±2	0.016
Bicuspid DT, ms	172±33	205±38	<0.001
Right ventricle			
FAC, %	44±4	50±4	<0.001
TAPSE, mm	16±3	24±2	<0.001
Tricuspid S', cm/s	11±3	13±2	<0.001
Tricuspid E, m/s	0.6±0.1	0.5±0.1	0.072
Tricuspid e', cm/s	10±3	11±3	0.047
Tricuspid E/e'	7±3	5±2	0.003

Data are expressed as mean±SD;  $P<0.05$  was considered statistically significant. BSA indicates body surface area; DBP, diastolic blood pressure; DT, deceleration time of E; FAC, fractional area change; HR, heart rate; HT, heart transplant; LVEF, left ventricular ejection fraction; SBP, systolic blood pressure; and TAPSE, tricuspid annular plane systolic excursion.

## Biventricular Functions by 3D-STE

HT group 3D-LVEF and RVEF values had decreased compared with the control values ( $P<0.001$ ), but remained within the normal range; 3D-myocardial strain values, LV GLS, LV GCS, LV GRS, and RV FWLS, were decreased in the HT group compared with those in the control group ( $P<0.001$ ; Table 3). The representative 3D-STE images for the abovementioned biventricular strain values between an HT recipient and a healthy control are illustrated in Figure 1.

Also, LVGS, LV twist, and torsion were lower in the HT group than those in the control group ( $P<0.001$ ). The HT group showed increased LV SDI compared with the control group ( $7.9\pm 2.2\%$  versus  $5.0\pm 1.6\%$ ,  $P<0.001$ ), but still within the normal range. Furthermore, the LV GPI (GPI=global peak systolic strain×torsion÷SDI) was decreased in the HT group than in the control group ( $P<0.001$ ) (Table 3). Moreover, the differences for LV GLS, LV GCS, LV GRS, LV GPI, and RV FWLS remained significant after adjustment for heart rate (Table S2). Furthermore, the values of LV GLS, LV GCS, LV GRS, LV GPI, and RV FWLS were entered into the receiver operating characteristic curve for detecting clinically well HT recipients, and the corresponding cutoff values, sensitivity, and specificity were determined. The biventricular strain values were all good for

**Table 3. Three-Dimensional Speckle-Tracking Echocardiographic Measurements of HT Group and Control Group**

Parameter	HT Group (n=46)	Control Group (n=46)	P Value
Left ventricle			
LVEF, %	62.5±4.4	67.8±4.1	<0.001
GS, %	-37.2±4.3	-41.3±4.0	<0.001
GLS, %	-17.2±1.3	-20.8±1.7	<0.001
GCS	-31.9±4.3	-36.8±4.0	<0.001
GRS	40.7±4.0	48.1±4.1	<0.001
Radial displacement, mm			
Septal	3.7±1.6	7.2±1.4	<0.001
Lateral	8.4±2.0*	6.2±1.1*	<0.001
Twist, °	13.3±5.2	18.2±5.5	<0.001
Torsion, °/cm	1.9±0.8	2.4±0.8	0.001
SDI, %	7.9±2.2	5.0±1.6	<0.001
GPI, °/cm	-10.4±7.5	-22.0±10.9	<0.001
Right ventricle			
RVEF, %	46.0±3.7	47.8±3.0	0.011
RV FWLS, %	-18.7±1.6	-22.1±2.0	<0.001

Data are expressed as mean±SD;  $P<0.05$  was considered statistically significant. FWLS indicates free wall longitudinal strain; GCS, global circumferential strain; GLS, global longitudinal strain; GPI, global performance index; GRD, global radial strain; GS, global peak systolic strain; HT, heart transplant; LVEF, left ventricular ejection fraction; RVEF, right ventricular ejection fraction; and SDI, systolic dyssynchrony index.

\*vs septal radial displacement,  $P<0.05$ .

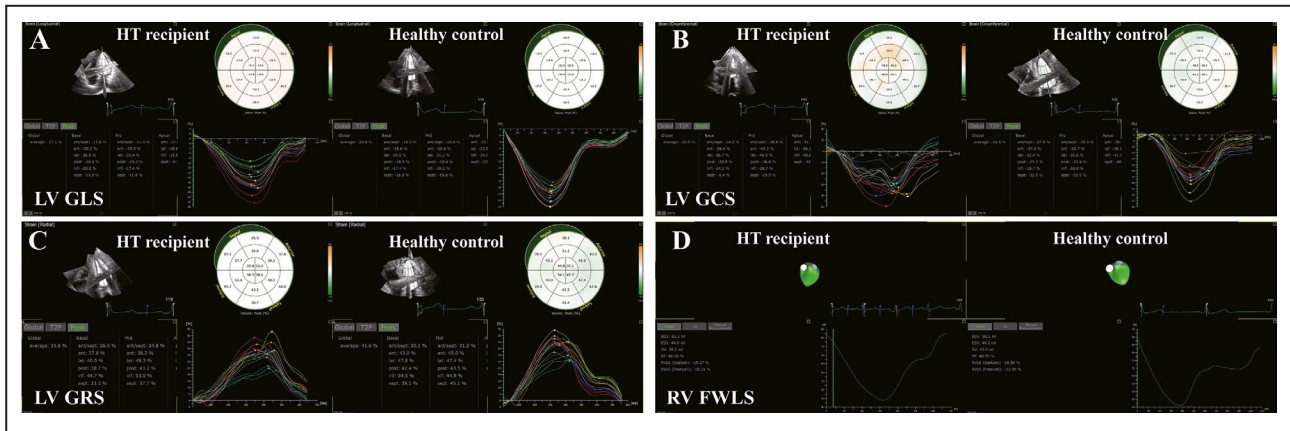


**Figure 1. Representative images for the comparison of biventricular mechanical function in a heart transplant recipient and a healthy control by 3-dimensional speckle-tracking echocardiography.**

Three-dimensional speckle-tracking echocardiography images for the reduced (A) left ventricular global longitudinal strain, (B) left ventricular global circumferential strain, (C) left ventricular global radial strain, and (D) right ventricular free wall longitudinal strain in a heart transplant recipient than that in healthy controls. 3D-STE indicates 3-dimensional speckle-tracking echocardiography; HT, heart transplant; LV GCS, left ventricular global circumferential strain; LV GLS, left ventricular global longitudinal strain; LV GRS, left ventricular global radial strain; and RV FWLS, right ventricular free wall longitudinal strain.

differentiating between the clinically well HT patients and non-HT healthy controls (the complete data are summarized in Figure 2).

### Left Ventricular Radial Displacement by 3D-STE

Compared with the control group, LV lateral wall radial displacement was higher, and septal wall radial displacement was reduced ( $P < 0.001$ ) in the HT group. And the LV radial displacement of the lateral wall was higher than that of the septal wall in the HT group ( $P < 0.001$ ), whereas the LV radial displacement of the lateral wall was lower than that of the septal wall in the control group ( $P < 0.001$ ) (Table 3).

### Reproducibility of 3D-STE and CMR

The measurements obtained by 3D-STE and CMR all showed excellent reproducibility. And the complete data of inter-observer variability and intra-observer variability were shown in Table 4.

## DISCUSSION

To the best of our knowledge, this is the first study comprehensively describing the characteristics and normal values for 3D-biventricular mechanical functions in a clinically well HT population. The results of this study suggest that (1) 3D-STE reveals excellent accuracy in the evaluation of biventricular functions in transplanted hearts against CMR; (2) the 3D-biventricular myocardial functions are significantly reduced even in clinically well HT recipients than control subjects.

Orthotopic HT involves numerous factors that affect myocardial function, making the graft ventricular function different from the control subjects even in healthy HT recipients. So, accurate evaluation of graft ventricular function is vital during the follow-up examinations. Previous studies, based on 2D echocardiography, have reported the normal LVEF and RV fractional area change, but reduction in LV GLS and RV FWLS in clinically stable HT recipients.<sup>9,10,21</sup> However, to the best of our knowledge, a study aiming at assessing the characteristics and normal values of biventricular mechanical functions in transplanted hearts using 3D-STE has not been reported. More importantly, 2D-STE is time-consuming, and the 2D plane of interest disappears during a cardiac cycle during the analysis. Moreover, the ventricular function derived from 2D echocardiography is dependent on geometric assumptions. Fortunately, 3D-STE could overcome these limitations for a more accurate and quick assessment of ventricular function.<sup>13,22</sup> In the present study, first, we validated the accuracy of 3D-STE in evaluating biventricular function against CMR in HT participants, which was consistent with previous studies in various other heart diseases.<sup>14–17</sup> Then, we further demonstrated the decreased 3D-biventricular myocardial strain, even in clinically well HT recipients with relatively normal 3D-ejection fraction. And these biventricular myocardial strain values (LV GLS, LV GCS, LV GRS, LV GPI, and RV FWLS) were all good for differentiating between clinically well HT patients and non-HT healthy controls.

Injury caused by ischemia-reperfusion, pericardiotomy surgery, subsequent progressive remodeling (including myocardial fibrosis, fibrous atrophy), and the

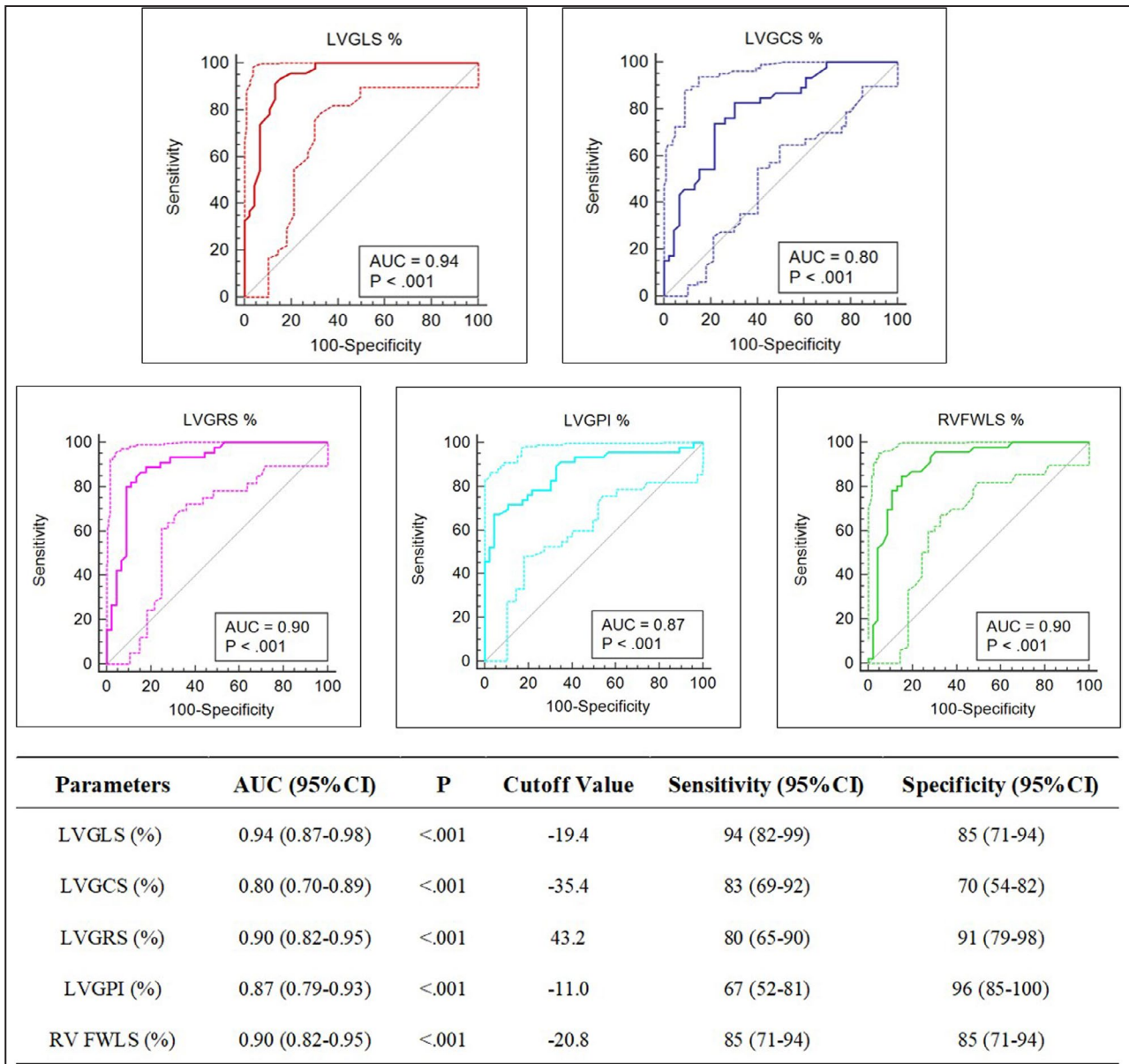


**Figure 2.** Receiver operating characteristic analysis for left ventricular (LV) global longitudinal strain, LV global circumferential strain, LV global radial strain, LV global performance index, and right ventricular free wall longitudinal strain. The area under the curve, best cutoff values, corresponding sensitivity, and the specificity for LV global longitudinal strain, LV global circumferential strain, LV global radial strain, LV global performance index, right ventricular free wall longitudinal strain are shown in the table below. AUC indicates area under the curve; LV GCS, left ventricular global circumferential strain; LV GLS, left ventricular global longitudinal strain; LV GPI, left ventricular global performance index; LV GRS, left ventricular global radial strain; and RV FWLS, right ventricular free wall longitudinal strain. Dashed lines representing 95% CI.

long-term therapy with immunosuppressants postoperatively can all result in the impairment of LV GLS.<sup>2-4</sup> Moreover, postoperative complications, including hypertension and diabetes mellitus, can also injure the myocardial functioning of the allograft. The studies on LV GCS in HT patients are relatively sparse, and the conclusions were controversial.<sup>9-11</sup> The LV GCS was reduced in our study that was consistent with the study by Marcello Chinali et al. Additionally, studies evaluating GRS in transplanted hearts are extremely

rare. LV twist function provides a key mechanistic link between cardiac systolic and diastolic functions, and it was sensitively affected by sympathetic stimulation.<sup>23,24</sup> Accordingly, the denervation in transplanted hearts could damage the twist dynamics. The impaired LV twist dynamics in our study were consistent with previous studies that were assessed using 2D-STE.<sup>25</sup> Additionally, this study reported higher (but still within normal range) LV SDI in transplanted hearts, which is consistent with a previous study.<sup>9</sup> The disproportion

**Table 4. Inter-Observer and Intra-Observer Reproducibility for the Parameters of 3-Dimensional Speckle-Tracking Echocardiography**

	ICC (95% CI)	Bias	LOA
Inter-observer (n=15)			
3D-LVEF (%)	0.97 (0.93–0.99)	–0.1	±2.4
3D-RVEF (%)	0.92 (0.72–0.98)	–1.3	±2.4
3D-LV GLS (%)	0.85 (0.66–0.95)	–0.7	±1.5
3D-LV GCS (%)	0.92 (0.79–0.97)	0.3	±3.9
3D-LV GRS (%)	0.93 (0.81–0.98)	0.3	±3.7
3D-RV FWLS (%)	0.86 (0.82–0.98)	–0.9	±2.7
CMR-LVEF (%)	0.96 (0.86–0.99)	–1.1	±3.4
CMR-RVEF (%)	0.93 (0.81–0.98)	0.5	±4.1
Intra-observer (n=15)			
3D-LVEF (%)	0.98 (0.94–0.99)	0.3	±1.6
3D-RVEF (%)	0.95 (0.86–0.98)	0.1	±2.7
3D-LV GLS (%)	0.88 (0.70–0.96)	0.7	±0.9
3D-LV GCS (%)	0.96 (0.89–0.99)	0.1	±2.2
3D-LV GRS (%)	0.97 (0.90–0.99)	–0.1	±2.1
3D-RV FWLS (%)	0.95 (0.85–0.98)	0.1	±1.9
CMR-LVEF (%)	0.98 (0.91–0.99)	0.9	±1.9
CMR-RVEF (%)	0.96 (0.89–0.99)	0.4	±2.9

3D indicates 3-dimensional; CMR, cardiac magnetic resonance; ICC, intra-class correlation coefficients; LOA, limits of agreement; LVEF, left ventricular ejection fraction; LV GCS, left ventricular global circumferential strain; LV GLS, left ventricular global longitudinal strain; LV GRS, left ventricular global radial strain; RV FWLS, right ventricular free wall longitudinal strain; and RVEF, right ventricular ejection fraction.

between the large size of recipient mediastinal cavity and small size of the donor's heart, as well as loss of support provided by the pericardial sac, may all increase the LV systolic dyssynchrony.<sup>26,27</sup> However, the abovementioned LV-myocardial strain and twist function could only assess individual aspects of the LV mechanical function. GPI, the new 3D-STE parameter which simultaneously incorporated the LV strain, torsion, and dyssynchrony, could reflect the comprehensive index of spatial movement and represent the global performance of LV.<sup>19</sup> This study further evaluated and illustrated the decrease in GPI after HT because GPI integrated the reduction in LV strain, twist, and the increase in LV systolic dyssynchrony.

Additionally, the reduced RV longitudinal function in HT recipients was similar to previous studies using 2D-STE.<sup>10,28</sup> Since cardiac surgery itself and complete pericardiectomy could cause the decreased RV longitudinal contraction and increased radial contraction simultaneously.<sup>5,29–31</sup> Therefore, transplanted hearts showed the reduced RV longitudinal function (not only the 3D-STE parameter-RV FWLS but also the conventional parameters including tricuspid annular plane systolic excursion and systolic tricuspid lateral annular tissue velocity) and normal overall contraction (including 2D-RV fractional area change and 3D-RVEF).

Our study further showed increased radial displacement of the lateral wall and decreased radial displacement of the septal wall in transplanted hearts. The disproportion between the large size of recipient mediastinal cavity and the small size of the donor's heart, as well as loss of support provided by the pericardial sac, may have enhanced the translational motion in transplanted hearts during the cardiac cycle.<sup>26,27</sup> The exaggerated translational motion mainly impacted the free wall of the allograft hearts, and it often showed a striking rightward and anterior movement during systole.<sup>32</sup> Accordingly, transplanted hearts showed increased lateral wall radial displacement and decreased septal wall radial displacement. Importantly, this validated phenomenon of marked translational motion aggravated the “out of plane phenomenon” associated with 2D-STE and strengthened the functionality of 3D-STE in graft hearts. Therefore, it is crucial to accurately describe the characteristics and appropriate normal values of biventricular mechanical functions via 3D-STE in transplanted hearts. And the definite characteristics and appropriate normal values of 3D-biventricular mechanical functions can provide a basis for evaluation and detection of ventricular dysfunction in follow-ups and further studies in transplanted hearts.

## Limitations

This was a single-center study, and the sample size was relatively small. Our study was limited to explore the normal 3D-biventricular mechanical functions in HT participants at 1-year post-surgery. Furthermore, 3D-STE was dependent on image quality. Moreover, the comparability of STE among different vendors is uncertain.

## CONCLUSIONS

This study validates that 3D-STE shows excellent accuracy in the evaluation of biventricular functions in transplanted hearts against CMR. HT patients who were considered clinically well show differences in their 3D-biventricular functions compared with those in non-HT healthy subjects. The 3D-biventricular mechanical functions are reduced in HT recipients. The provided characteristics and appropriate normal values of biventricular mechanical functions can be the basis for accurate evaluation and detection of ventricular dysfunction in follow-up examinations and further studies in the transplanted hearts.

## ARTICLE INFORMATION

Received December 22, 2019; accepted March 27, 2020.

### Affiliations

From the Departments of Ultrasound (Q.L., W.S., J.W., C.W., H.L., Y.L., L.Z., M.X.), Radiology (X.S., B.L.), and Cardiovascular Surgery (N.D.), Union



Hospital, Tongji Medical College, Huazhong University of Science and Technology, Wuhan, China; Hubei Province Key Laboratory of Molecular Imaging, Wuhan, China (Q.L., W.S., J.W., C.W., H.L., Y.L., L.Z., M.X.).

### Acknowledgments

The authors thank Jie Cai, MD, PhD and Jing Zhang, MD for their assistance with the management of HT patients, and Ping Yin, PhD for his assistance in statistical analysis.

### Sources of Funding

This work was supported by the National Natural Science Foundation of China (grant numbers: 81922033, 81530056, 81671705, 81727805, 81771851) and the National Key Research and Development Program of China (grant number: 2018YFC0114600).

### Disclosures

None.

### Supplementary Materials

Tables S1–S2

Figures S1–S2

## REFERENCES

- Lund LH, Edwards LB, Dipchand AI, Goldfarb S, Kucheryavaya AY, Levvey BJ, Meiser B, Rossano JW, Yusef RD, Stehlik J. The Registry of the International Society for Heart and Lung Transplantation: thirty-third adult heart transplantation report—2016; focus theme: primary diagnostic indications for transplant. *J Heart Lung Transplant.* 2016;35:1158–1169.
- Linfert D, Chowdhry T, Rabb H. Lymphocytes and ischemia-reperfusion injury. *Transplant Rev (Orlando).* 2009;23:1–10.
- Nozynski J, Zakliczynski M, Zembala-Nozynska E, Konecka-Mrowka D, Przybylski R, Nikiel B, Lange D, Mrówka A, Przybylski J, Maruszewski M, et al. Remodeling of human transplanted myocardium in ten-year follow-up: a clinical pathology study. *Transplant Proc.* 2007;39:2833–2840.
- Appleyard RF, Cohn LH. Myocardial stunning and reperfusion injury in cardiac surgery. *J Card Surg.* 1993;8:316–324.
- Raina A, Vaidya A, Gertz ZM, Susan C, Forfia PR. Marked changes in right ventricular contractile pattern after cardiothoracic surgery: implications for post-surgical assessment of right ventricular function. *J Heart Lung Transplant.* 2013;32:777–783.
- Badano LP, Miglioranza MH, Edvardsen T, Colafranceschi AS, Muraru D, Bacal F, Nieman K, Zoppellaro G, Marcondes Braga FG, Binder T, et al. European Association of Cardiovascular Imaging/Cardiovascular Imaging Department of the Brazilian Society of Cardiology recommendations for the use of cardiac imaging to assess and follow patients after heart transplantation. *Eur Heart J Cardiovasc Imaging.* 2015;16:919–948.
- Clemmensen TS, Logstrup BB, Eiskjaer H, Poulsen SH. Serial changes in longitudinal graft function and implications of acute cellular graft rejections during the first year after heart transplantation. *Eur Heart J Cardiovasc Imaging.* 2016;17:184–193.
- Clemmensen TS, Logstrup BB, Eiskjaer H, Poulsen SH. Evaluation of longitudinal myocardial deformation by 2-dimensional speckle-tracking echocardiography in heart transplant recipients: relation to coronary allograft vasculopathy. *J Heart Lung Transplant.* 2015;34:195–203.
- Saleh HK, Villarraga HR, Kane GC, Pereira NL, Raichlin E, Yu Y, Koshino Y, Kushwaha SS, Miller FA Jr, Oh JK, et al. Normal left ventricular mechanical function and synchrony values by speckle-tracking echocardiography in the transplanted heart with normal ejection fraction. *J Heart Lung Transplant.* 2011;30:652–658.
- Ingvarsson A, Werther Ewaldsson A, Waktare J, Nilsson J, Smith GJ, Stagno M, Roijer A, Rådegran G, Meurling CJ. Normal reference ranges for transthoracic echocardiography following heart transplantation. *J Am Soc Echocardiogr.* 2018;31:349–360.
- Chinali M, Esposito C, Grutter G, Iacobelli R, Toscano A, D'Asaro MG, Del Pasqua A, Brancaccio G, Parisi F, Drago F, et al. Cardiac dysfunction in children and young adults with heart transplantation: a comprehensive echocardiography study. *J Heart Lung Transplant.* 2017;36:559–566.
- Urbano-Moral JA, Arias-Godinez JA, Ahmad R, Malik R, Kiernan MS, DeNofrio D, Pandian NG, Patel AR. Evaluation of myocardial mechanics with three-dimensional speckle tracking echocardiography in heart transplant recipients: comparison with two-dimensional speckle tracking and relationship with clinical variables. *Eur Heart J Cardiovasc Imaging.* 2013;14:1167–1173.
- Saito K, Okura H, Watanabe N, Hayashida A, Obase K, Imai K, Maehama T, Kawamoto T, Neishi Y, Yoshida K. Comprehensive evaluation of left ventricular strain using speckle tracking echocardiography in normal adults: comparison of three-dimensional and two-dimensional approaches. *J Am Soc Echocardiogr.* 2009;22:1025–1030.
- Dorosz JL, Lezotte DC, Weitzenkamp DA, Allen LA, Salcedo EE. Performance of 3-dimensional echocardiography in measuring left ventricular volumes and ejection fraction: a systematic review and meta-analysis. *J Am Coll Cardiol.* 2012;59:1799–1808.
- Bell A, Rawlins D, Bellsham-Revell H, Miller O, Razavi R, Simpson J. Assessment of right ventricular volumes in hypoplastic left heart syndrome by real-time three-dimensional echocardiography: comparison with cardiac magnetic resonance imaging. *Eur Heart J Cardiovasc Imaging.* 2014;15:257–266.
- Muraru D, Spadotto V, Cecchetto A, Romeo G, Aruta P, Ermacora D, Jeneli C, Cucchini U, Iliceto S, Badano LP. New speckle-tracking algorithm for right ventricular volume analysis from three-dimensional echocardiographic data sets: validation with cardiac magnetic resonance and comparison with the previous analysis tool. *Eur Heart J Cardiovasc Imaging.* 2016;17:1279–1289.
- Tsang W, Salgo IS, Medvedofsky D, Takeuchi M, Prater D, Weinert L, Yamat M, Mor-Avi V, Patel AR, Lang RM. Transthoracic 3D Echocardiographic Left Heart Chamber Quantification Using an Automated Adaptive Analytics Algorithm. *JACC Cardiovasc Imaging.* 2016;9:769–782.
- Lang RM, Badano LP, Mor-Avi V, Afilalo J, Armstrong A, Ernande L, Flachskampf FA, Foster E, Goldstein SA, Kuznetsova T, et al. Recommendations for cardiac chamber quantification by echocardiography in adults: an update from the American Society of Echocardiography and the European Association of Cardiovascular Imaging. *Eur Heart J Cardiovasc Imaging.* 2015;28:1–39.
- Yu HK, Yu W, Cheuk DK, Wong SJ, Chan GC, Cheung YF. New three-dimensional speckle-tracking echocardiography identifies global impairment of left ventricular mechanics with a high sensitivity in childhood cancer survivors. *J Am Soc Echocardiogr.* 2013;26:846–852.
- Kapetanakis S, Kearney MT, Siva A, Gall N, Cooklin M, Monaghan MJ. Real-time three-dimensional echocardiography: a novel technique to quantify global left ventricular mechanical dyssynchrony. *Circulation.* 2005;112:992–1000.
- Eleid MF, Caracciolo G, Cho EJ, Scott RL, Steidley DE, Wilansky S, Arabia FA, Khandheria BK, Sengupta PP. Natural history of left ventricular mechanics in transplanted hearts: relationships with clinical variables and genetic expression profiles of allograft rejection. *JACC Cardiovasc Imaging.* 2010;3:989–1000.
- Seo Y, Ishizu T, Atsumi A, Kawamura R, Aonuma K. Three-dimensional speckle tracking echocardiography. *Circ J.* 2014;78:1290–1301.
- Stohr EJ, Shave RE, Baggish AL, Weiner RB. Left ventricular twist mechanics in the context of normal physiology and cardiovascular disease: a review of studies using speckle tracking echocardiography. *Am J Physiol Heart Circ Physiol.* 2016;311:H633–H644.
- Hansen DE, Daughters GT II, Alderman EL, Ingels NB, Stinson EB, Miller DC. Effect of volume loading, pressure loading, and inotropic stimulation on left ventricular torsion in humans. *Circulation.* 1991;83:1315–1326.
- Cameli M, Ballo P, Lisi M, Benincasa S, Focardi M, Bernazzali S, Lisi G, Maccherini M, Henein M, Mondillo S. Left ventricular twist in clinically stable heart transplantation recipients: a speckle tracking echocardiography study. *Int J Cardiol.* 2013;168:357–361.
- Feneley M, Kearney L, Farnsworth A, Shanahan M, Chang V. Mechanisms of the development and resolution of paradoxical interventricular septal motion after uncomplicated cardiac surgery. *Am Heart J.* 1987;114:106–114.
- D'Souza KA, Mooney DJ, Russell AE, Maclsaac AI, Aylward PE, Prior DL. Abnormal septal motion affects early diastolic velocities at the septal and lateral mitral annulus, and impacts on estimation of the pulmonary capillary wedge pressure. *J Am Soc Echocardiogr.* 2005;18:445–453.
- Lakatos BK, Tokodi M, Assabiny A, Tószér Z, Kosztin A, Doronina A, Racz K, Koritsanszky KB, Berzsényi V, Nemeth E, et al. Dominance of free wall radial motion in global right ventricular function of heart transplant recipients. *Clin Transplant.* 2018;32:e13192.

- 
29. Unsworth B, Casula RP, Kyriacou AA, Yadav H, Chukwuemeka A, Cherian A, de Lisle Stanbridge R, Athanasiou T, Mayet J, Francis DP. The right ventricular annular velocity reduction caused by coronary artery bypass graft surgery occurs at the moment of pericardial incision. *Am Heart J*. 2010;159:314–322.
  30. Fritz T, Wieners C, Seemann G, Steen H, Dossel O. Simulation of the contraction of the ventricles in a human heart model including atria and pericardium. *Biomech Model Mechanobiol*. 2014;13:627–641.
  31. White BR, Katcoff H, Faerber JA, Lin KY, Rossano JW, Mercer-Rosa L, O'Connor MJ. Echocardiographic assessment of right ventricular function in clinically well pediatric heart transplantation patients and comparison with normal control subjects. *J Am Soc Echocardiogr*. 2019;32:537–544.
  32. Dandel M, Hetzer R. Post-transplant surveillance for acute rejection and allograft vasculopathy by echocardiography: usefulness of myocardial velocity and deformation imaging. *J Heart Lung Transplant*. 2017;36:117–131.

# **SUPPLEMENTAL MATERIAL**

**Table S1. Clinical Characteristics of the 35 HT Recipients in Protocol 1.**

<b>Parameter</b>	<b>Value</b>
Men (%)	27 (78%)
Age (years)	45±14
Height (cm)	166±8
Weight (kg)	63±14
BSA (m <sup>2</sup> )	1.7±0.2
SBP (mmHg)	120±12
DBP (mmHg)	79±9
HR (bpm)	89±7
Time since HT (months)	19±9
Clinical status	
Clinically well	28(80%)
ACR	4(11%)
CAV	2(6%)
Lymphoproliferative disease	1(3%)

Data are expressed as mean ± SD or as number (%). ACR, acute rejection; CAV, cardiac allograft vasculopathy; DBP, diastolic blood pressure; HT, heart transplant; SBP, systolic blood pressure.

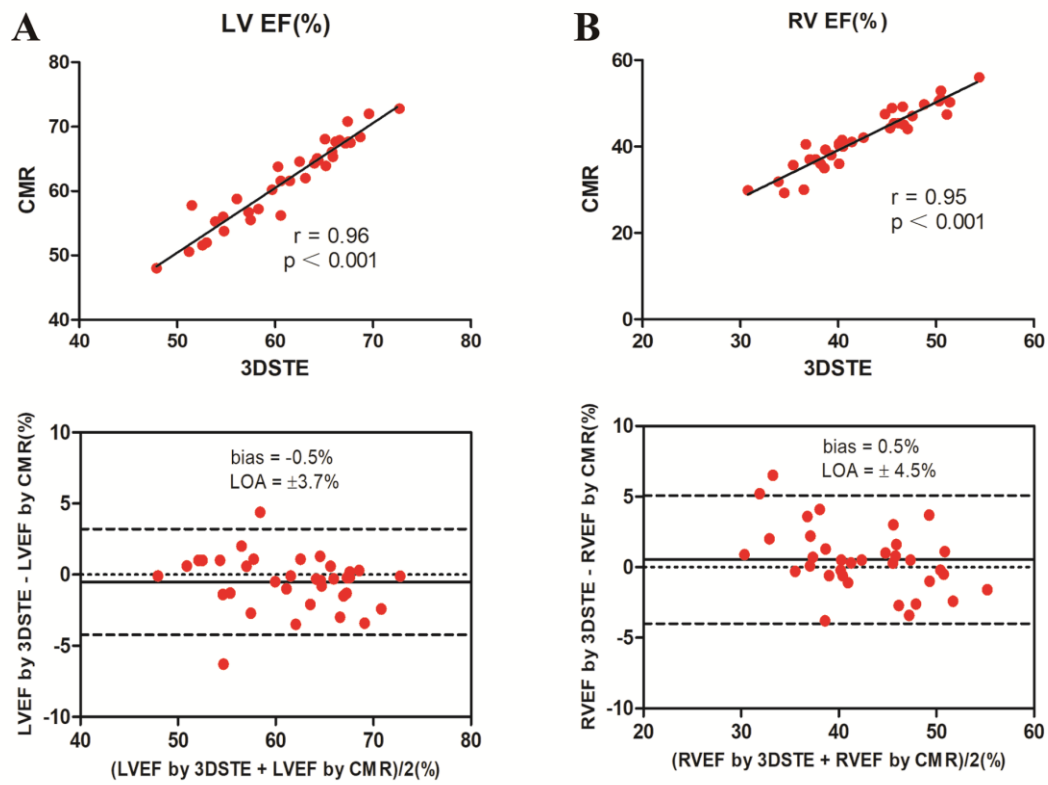


**Table S2. The Adjustment of the Comparisons of Three-Dimensional Speckle-Tracking Echocardiographic Measures between HT Group and Control Group.**

Parameter	HT Group (n=46)	Control Group (n=46)	P value
<b>Left Ventricle</b>			
LVEF (%)	62.3 (60.7 to 63.8)	68.1 (66.5 to 70.0)	<0.001
GS (%)	-37.0 (-35.4 to -38.5)	-41.5 (-39.9 to -43.0)	0.01
GLS (%)	-17.4 (-18.0 to -16.9)	-20.6 (-21.1 to -20.0)	<0.001
GCS	-31.5 (-33.0 to -30.0)	-37.2 (-38.7 to -35.6)	<0.001
GRS	40.7 (39.2 to 42.2)	48.2 (46.7 to 50.0)	<0.001
Radial displacement (mm)			
Septal	3.6 (3.1 to 4.2)	7.2 (6.7 to 7.8)	<0.001
Lateral	8.4 (7.8 to 9.0) <sup>a</sup>	6.2 (5.6 to 6.8) <sup>*</sup>	<0.001
Twist (°)	13.9 (11.9 to 15.8)	17.6 (15.7 to 19.6)	0.023
Torsion (°/cm)	1.9 (1.7 to 2.2)	2.4 (2.1 to 2.6)	0.088
SDI (%)	7.5 (6.8 to 8.2)	5.3 (4.6 to 6.0)	<0.001
GPI (°/cm)	-20.3 (-23.7 to -16.9)	-12.1 (-15.5 to -8.7)	0.005
<b>Right Ventricle</b>			
RVEF (%)	47.7 (46.5 to 48.9)	46.2 (45.0 to 47.4)	0.128
RV FWLS (%)	-19.0 (-19.6 to -8.3)	-21.9 (-22.6 to -21.2)	<0.001

Data are expressed as mean (95%CI); A p value<0.05 was considered statistically significant. <sup>\*</sup> vs septal radial displacement, p<0.05. FWLS, free wall longitudinal strain; GS, global peak systolic strain; GLS, global longitudinal strain; GCS, global circumferential strain; GRS, global radial strain; GPI, global performance index; HT, heart transplant; LVEF, left ventricular ejection fraction; RVEF, right ventricular ejection fraction; SDI, systolic dyssynchrony index.

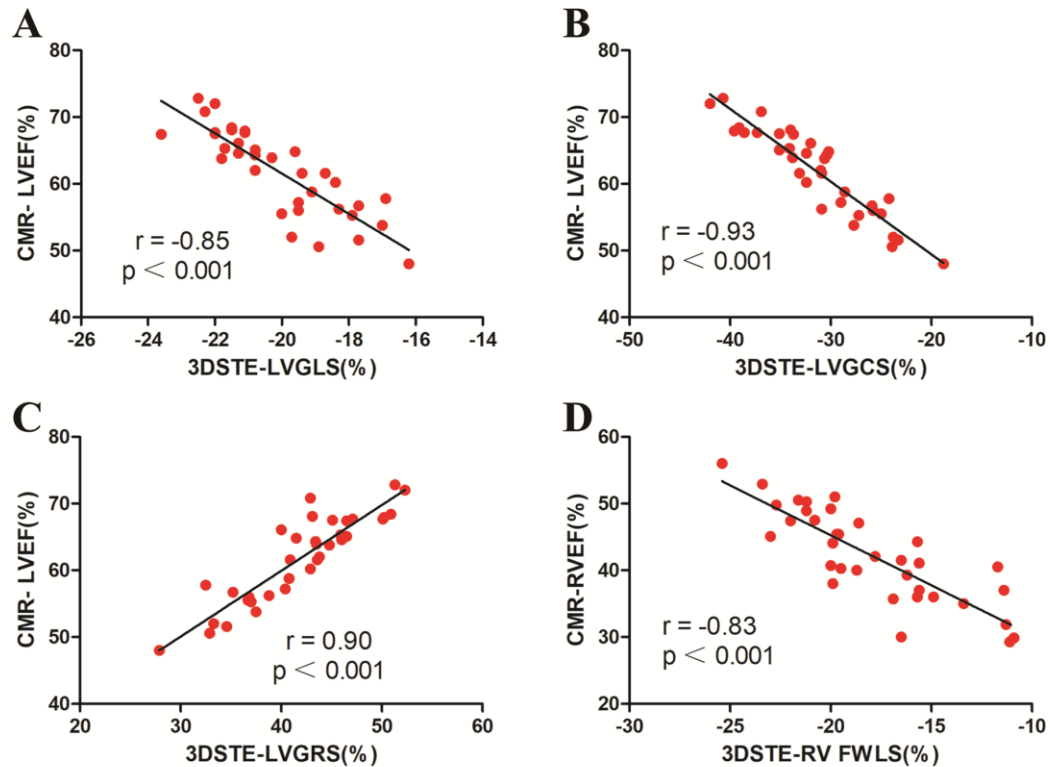
**Figure S1. Accuracy of 3D-STE against CMR for evaluating biventricular EF in HT recipients.**



Correlation (top) and Bland-Altman analysis (bottom) of (A, LVEF) and (B, RVEF).

3D-STE, three-dimensional speckle-tracking echocardiography; CMR, cardiac magnetic resonance; HT, heart transplant; LVEF, left ventricular ejection fraction; LOA, limits of agreement; RVEF, right ventricular ejection fraction.

**Figure S2. Linear correlation between myocardial strain values by 3D-STE and CMR-EF in HT recipients.**



(A, LVGLS), (B, LVGCS), (C, LVGRS) by 3D-STE correlated well with CMR-LVEF; (D, RV FWLS) by 3D-STE correlated well with CMR-RVEF.

3D-STE, three-dimensional speckle-tracking echocardiography; CMR, cardiac magnetic resonance; HT, heart transplant; LVEF, left ventricular ejection fraction; LVGLS, left ventricular global longitudinal strain; LVGCS, left ventricular global circumferential strain; LVGRS, left ventricular global radial strain; RVEF, right ventricular ejection fraction; RV FWLS, right ventricular free wall longitudinal strain.